CHAPTER II
THEORY AND LITERATURES REVIEW

2.1 Molecular sieve dehydrator – the early days

The equipment used during the early stage of the fuel ethanol program was built using a combination of technologies borrowed from different industries. Most of the basic production expertise came from the beverage alcohol industry, but there were no need to remove all the water from beverage alcohol. To prevent phase separation when blended with gasoline, fuel grade ethanol needed to be almost completely dry. Standard distillation still leaves over 4% water in the ethanol, so a process called azeotropic distillation was used in all the early commercial ethanol plants to remove the final water from the ethanol. Azeotropic distillation uses a third component, typically benzene or cyclohexane, to break the azeotrope (Gomis *et al.*, 2007).

Azeotropic distillation systems tended to be quite expensive, difficult to operate and adjust, and consumed a significant amount of energy. Attempts were made to reduce the operating difficulties and energy consumption, but the two goals were incompatible. Multi-pressure techniques could reduce energy consumption, but at the expense of more difficult operation and considerably higher capital cost (Modla and Lang, 2008). A process upset could easily contaminate the ethanol product with benzene.

In 1957 an inventor name Skarstrom received a patent for a device that utilized a synthetic zeolite adsorbent that selectively removed water from air and some other gases and vapors. A different zeolite could even be used in virtually the same device to separate oxygen and nitrogen from air (Ruthven, 1984). These synthetic zeolites became known as molecular sieves due to the very precise pore size that enabled them to select and remove one molecular size from a bulk mixture containing molecules with a larger size or lower polarity. When adsorption of water on zeolite was initially introduced into the ethanol industry, there were problems with desiccant fouling and high energy consumption especially with the liquid phase

system. Not only until late 80's that the technology had proven to be a success in an industrial scale. Molecular sieve dehydrator offered the industry lower capital costs, lower operating costs, and greater personnel safety than azeotropic distillation.

2.2 Pressure swing adsorption

Most modern molecular sieve dehydrators use a process known in the industry as pressure swing adsorption to remove water from a vaporized feed stream. The term pressure swing refers to the fact that the dehydrator uses a relatively high pressure stream when water is being removed from the feed stream and a relatively low pressure when the molecular sieve desiccant is being regenerated. Most commercial designs have two or more beds of desiccant and cycle the vapor flow through the beds to provide continuous operation. While one bed is on-line drying the feed vapor, another bed is being regenerated. In some designs one or more additional beds are being depressurized or repressurized in preparation for the next cycle (Le Van, 1996).

The macroscopic principles of adsorption are quite simple, but attempts to accurately explain how adsorption works often fail. The basic characteristic of an adsorbent material is a stronger affinity for one type of atom or molecule than for the other types in the vapor stream. In the case of a molecular sieve ethanol dehydrator, an adsorbent with a strong affinity for water and little affinity for ethanol and the other impurities typically contained in the ethanol feed stream is selected. As wet ethanol vapor passes through the bed, the desiccant adsorbs the water molecules but not the ethanol molecules. This process cannot continue definitely, because the desiccant has a finite capacity for water and that capacity is affected by the operating temperature and pressure. Moisture capacity increases as pressure increases or temperature decreases, and vice versa. Since a pressure swing adsorption dehydrator operates at almost constant temperature (Ruthven *et al.*, 1994), the system can desorb the water adsorbed on the previous cycle by lowering the operating pressure and passing a purge vapor through the bed in the opposite direction to sweep the water molecules from the free space surrounding the desiccant beads.

The class of materials known as zeolites occurs naturally, but most commercial molecular sieves are man-made. Synthetic zeolites have a crystalline lattice structure that contains openings (pores) of a precise size, usually measured in angstroms (Å). Molecular sieves can be manufactured with different pore sizes by using different chemistry and different preparation methods. A synthetic zeolite of type 3A is used in most ethanol dehydrators, because the pores are 3 Å in diameter while water molecules are 2.8 Å and ethanol molecules are 4.4 Å. Therefore, water molecules are strongly attracted into the pores but ethanol molecules are excluded. Many other adsorbent materials are available that have affinity for water such as activated alumina. However, other adsorbents have a wide range of pore sizes and therefore are much less selective than molecular sieves.

Water is so strongly attracted to type 3 A molecular sieve that for each kilogram adsorbed, 4,200 kJ of heat is released. This effect is referred to as the heat of adsorption. When removing that same kilogram of water during regeneration, 4,200 kJ of heat (referred to as heat of desorption) must be supplied. Thus, as feed vapor is dehydrated the bed of desiccant heats up and as the bed is regenerated it cools down. Type 3A molecular sieve is capable of adsorbing up to 22% of its weight in water, but pressure swing adsorption dehydrators operate at a much lower moisture loading and limit the dehydration period to prevent an excessive temperature swing.

2.3 A typical operating cycle described

By limiting the adsorption period, temperature swings are kept to a reasonable value and the heat of adsorption can be effectively stored in the bed of desiccant as sensible heat. The heat is then available to supply the necessary heat of desorption during the regeneration period. The ability to recover the heat of adsorption is why molecular sieve dehydrators are so energy efficient. Assuming the feed vapor comes directly from the rectifier column, the only energy used directly in the PSA system is the steam required to superheat the vapor to bed operating temperatures and the electricity to operate the pumps and other equipments. A properly design system will have a totally inclusive energy consumption of about 1,200 kJ per liter of anhydrous ethanol, assuming the feed ethanol contains 5% water and the product is dried to 0.25% water. Additional energy is required if the feed ethanol is wetter of if the

product is higher. Molecular sieve dehydrators can accommodate a wide range of specifications, and can be built for any desired production rate. Some are currently in service drying ethanol containing as much as 20% water and some can produce anhydrous ethanol with as little as 20 ppm water in the final product.

The following describes a typical operating cycle for a 2-bed dehydrator drying ethanol containing 5% water. At the beginning Bed 1 on-line (drying the feed vapor) and Bed 2 being regenerated (Figure 2.1). Wet ethanol vapor enters the top of Bed 1 under a modest pressure, passes downward through the bed and exits the bottom as dry vapor. Appoximately 60-85% of the vapor leaves the system as anhydrous ethanol product and the remainder is fed to Bed 2 as a regeneration purge stream. Bed 2 is maintained under a vacuum that shifts the equilibrium conditions so that the adsorbed water is desorbed. Operating pressures, temperatures and flow rates are adjusted so that regeneration is complete at the point in the cycle when the beds change position (valves are positioned to reverse the roles of the two beds). One bed typically stays on-line dehydrating the feed stream for 3-10 minutes before being regenerated. When the beds transition from dehydrate to regenerate mode, the pressure in the inlet header tends to sag, which can upset the rectifier column if provisions are not made to mitigate the pressure drop. After the beds switch, the bed that was being regenerated pressures up to the dehydrating pressure and the vacuum system lowers the pressure in the other bed to the regenerating pressure. The cycle repeats itself continuously. Since one bed or the other is always receiving and drying the inlet vapor, the process seems to be continuously but in reality it is more properly termed as 'cyclic batch' (Swain, 1999).

While a molecular sieve dehydrator can operate on a simple timed cycle, the best systems are managed by a controller to provide greater operating safety, reliability and energy efficiency. Once adjusted to standard operating conditions, the molecular sieve dehydrator requires little operator interface and can tolerate reasonable variations in feed rate or quality without need for readjustment. Typical quality control measures include sampling the product, feed and regeneration liquid at regular intervals to assure the product meets specifications and that the system is operating efficiently.

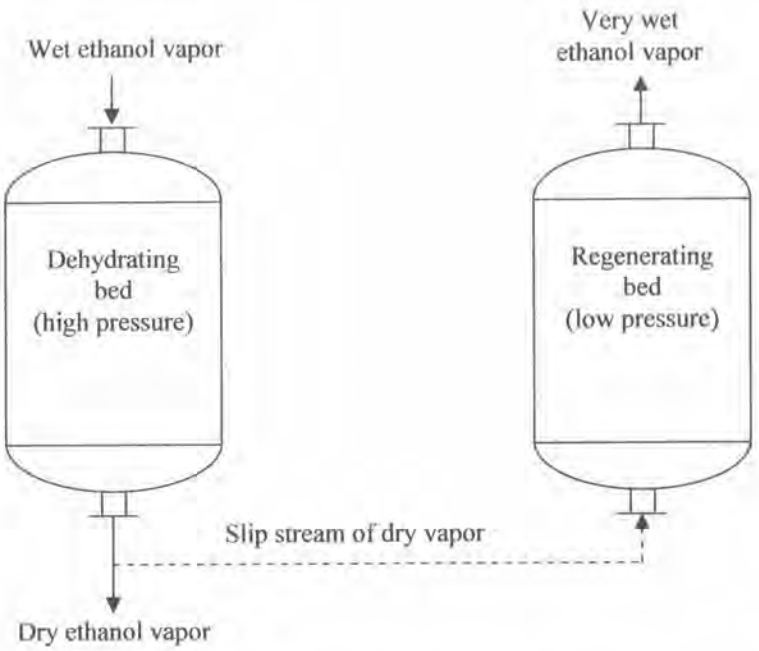

Figure 2.1 Operation of two bed molecular sieve dehydrator.

2.4 Zeolites

Zeolites or molecular sieves are nonporous oxide crystalline structures, typically aluminosilicates. The aluminum in the structure has a negative charge that must be balanced by a cation, M. This ionic structure leads to the hydrophilicity of the zeolite. Silicalite, a pure silica version, is charge neutral and hydrophobic. Zeolites have uniform pore sizes that typically range from 0.3 to 0.8 nm. The pore size and/or adsorption strength can be altered by the type and number of cations present in the structure. The void fraction can be as high as 0.5. Zeolites can selectively adsorb or reject molecules based on their size, shape, or sorption strength. The molecular sieving effect is a common term associated with zeolites, and refers to selectivity based on size or shape exclusion. Zeolites can also provide separations based on competitive sorption. This situation can lead to reverse selectivity where a larger molecule can be selectively adsorbed and separated from a smaller molecule. For example, most zeolites are polar adsorbents and will preferentially adsorb polar species over non-polar species of comparable size.

Noble and Terry (2004) suggest that separation can be based on the molecular sieve effect and selective adsorption. These separations are governed by several factors:

1. The basic framework structure of the zeolite determines the pore size and the void volume.

2. The exchange cations, in terms of their specific location in the structure, number density, charge, and size, affect the molecular sieve behavior and adsorption selectivity of the zeolite. By changing the cation type number, one can modify the selectivity if the zeolite fir a given separation.

3. The effect of the temperature can be substantial in situations involving activated diffusion.

Many zeolites occur naturally but the majority of those used commercially have been synthesized and are designated by a letter or group of letters (Type A, Type Y, Type ZSM, etc.). The lettering system has evolved empirically and has no relation to the structure. Tables 2.1, 2.2, and 2.3 list some industrial applications of adsorption operations, properties of adsorbents and their environmental applications.

Table 2.1 Industrial Applications of Sorption Operations (Seader and Henley, 1998)

1. Adsorption
   Gas purifications
   Gas bulk separations:
   N_2/O_2
   H_2O/ethanol
   Acetone/vent streams
   C_2H_4/vent streams
   Normal paraffins/isoparaffins, aromatics
   CO, CH_4, CO_2, N_2, A, NH_3/H_2
   Liquid purifications
   Liquid bulk separation
2. Ion Exchange
   Water softening
   Water demineralization
   Water dealkalization

Decolorization of sugar solutions

Recovery of antibiotics from fermentation broths

Recovery of vitamins from fermentation broths

3. Chromatography

Separation of sugars

Separation of perfumes

Separation of C_4-C_{10} normal and isoparaffins

Table 2.2 Representative Properties of Commercial Porous Adsorbents (Seader and Henley, 1998)

Adsorbent	Nature	Pore Diameter d_p, Å	Particle Porosity ε_p	Particle Density ρ_p, g/cm^3	Surface Area S_g, m^2/g	Capacity for H_2O Vapor at 25 °C and 4.6 mmHg, wt% (Dry Basis)
Activated alumina	Hydrophilic, amorphous	10-75	0.50	1.25	320	7
Silica gel:	Hydrophilic/					
Small pore	hydrophobic,	22-26	0.47	1.09	750-850	11
Large pore	amorphous	100-150	0.71	0.62	300-350	-
Activated carbon:	Hydrophobic, amorphous					
Small pore		10-25	0.4-0.6	0.5-0.9	400-1,200	1
Large pore		>30	-	0.6-0.8	200-600	-
Molecular sieve carbon	Hydrophobic	2-10	-	0.98	400	-
Molecular sieve zeolites	Polar-hydrophilic crystalline	3-10	0.2-0.5	-	600-700	20-25
Polymeric adsorbents	-	40-25	0.4-0.55	-	80-700	-

Table 2.3 Properties and Applications of Some Molecular Sieve Zeolites

Designation	Cation	Unite Cell Formula	Aperture Size, Å	Typical Application
3A	K^+	$K_{12}[(AlO_2)_{12}(SiO_2)_{12}]$	2.9	Drying of reactive gases
4A	Na^+	$Na_{12}[(AlO_2)_{12}(SiO_2)_{12}]$	3.8	H_2O/CO_2 removal; air separation
5A	Ca^{2+}	$Ca_5Na_2[(AlO_2)_{12}(SiO_2)_{12}]$	4.4	Separation of air; separation of linear paraffins
10X	Ca^{2+}	$Ca_{43}[(AlO_2)_{86}(SiO_2)_{106}]$	8	Separation of air;
13X	Na^+	$Na_{86}[(AlO_2)_{86}(SiO_2)_{86}]$	8.4	removal of mercaptans

2.5 Desorption and regeneration of adsorbents

In certain applications it may be economic to discard the adsorbent after use in which case it may be necessary to describe it as a waste. Clearly the nature and concentration of the adsorbates will dictate the disposal route to be followed. Disposal would be favored when the adsorbent is of low cost, is very difficult to regenerate (perhaps because adsorbates are held by chemical forces) and the no-adsorbed products of the adsorptive separation are of very high value. In the majority of process applications, disposal of the adsorbent as a waste is not an economic option and therefore regeneration is carried out either internal or external to the adsorption vessel to an extent sufficient that the adsorbent can be reused. Practical methods of desorption and regeneration include one, or more usually a combination, of the following:

1. increase in temperature;
2. reduction in partial pressure;
3. reduction in concentration;
4. purging with an inert fluid;
5. displacement with a more strongly adsorbing species;
6. change of chemical condition such as pH.

As a variable for changing thermodynamic potential, a change in temperature is much more effective than a change in pressure. However, the final choice of regeneration method depends upon technical and economic considerations. The most common methods are changes in pressure (pressure swing adsorption). The general

advantages and disadvantages of each method together with some process examples are shown in Table 2.4.

Table 2.4 Methods of regeneration with process examples (Ruthven 1984 and Crittenden 1992)

Method	Advantages	Disadvantages	Process	Adsorbent	Examples of use, selectivity
Thermal swing	Good for strongly adsorbed species Desorbate recovered at high concentrations For gases and liquids	Thermal ageing of sorbent Heat loss leads to thermal inefficiency Long cycle times mean inefficiency use of sorbent High latent heat for liquids	Drying of gases Drying of solvents	3A, 4A, 13X 4A	Equilibrium Equilibrium
Pressure swing	Good for weakly adorbed species required in high purity	Very low P may be required Mechanical energy more expensive than heat	Drying of gases Hydrogen recovery Air separation Air separation	3A, 4A, 13X Mol Sieve Carb mol sieve Zeolite	Equilibrium Equilibrium Kinetic Equilibrium
Vacuum (special case of pressure swing)	Rapid cycling gives efficient use of sorbent	Desorbate recovered at low purity	Separation of linear paraffins	5A mol sieve	Shape selective sieving
Displacement	Good for strongly helded species Avoids risk of cracking reactions during regenerations Avoids thermal ageing of sorbent	Product separation and recovery needed	Separation of linear from branched and cyclic paraffins	5A mol sieve	Shape selective sieving
Purge gas stripping	Essentially at constant T and P	Only for weakly sorbed species, purge flow is high Not normally used when desorbate needs to be recovered	Relatively uncommon without thermal swing since purging alone is only suitable for weakly adsorbed species		
Steam stripping (combination of thermal swing and displacement)	As for thermal swing and displacement above		Waste wacr purification Solvent recovery	Activated carbon	Equilibrium

2.6 Fixed bed processes

Separation in a fixed bed of adsorbent is, in virtually all practical cases, and unsteady state rate controlled process. This means that conditions at any particular point within the fixed bed vary with time. Adsorption therefore occurs only in a particular region of the bed, known as the mass transfer zone, which moves through the bed with time.

2.6.1 LUB Approach for Non Linear Systems

In general, analytical solutions of the complete mass and energy balances for nonlinear systems cannot be obtained. One exception to this is for isothermal systems when a constant pattern wave occurs. Constant pattern waves are concentration waves that do not change shape as they move down the column. They occur when the solute movement analysis predicts a shock wave.

Experimental results and the shock wave analysis of adsorption of water from ethanol/water mixture showed that the wave shape for constant pattern waves is independent of the distance traveled. This allows the analysis to be divided into two parts. First, the center of the wave can be determined by analyzing the shock wave with solute movement theory. Second, the partial differential equations for the column mass balance can be simplified to an ordinary differential equation by using a variable $= t - Z/u_{sh}$ that defines the deviation from the center of the wave. This approach is detailed in more advance literature sources.

A simplified analysis procedure called the Length of Unused Bed (LUB), or Mass Transfer Zone (MTZ), method that uses experimental data to design columns during constant pattern operation is used in the industry. This method is base on the work of Michaels (1952). The constant pattern wave inside the bed is shown schematically in Figure 2.2. After being fully developed, the pattern does not change as it moves through the bed. The width of this pattern (called the length of the MTZ, L_{MTZ}) is usually arbitrarily measured from 0.05 C_F to 0.95 C_F. The reason for not using zero or the feed concentration is it is very difficult to determine exactly when these values are left or attained. During operation, the feed step is stopped at t_{br} when

the outlet concentration reaches a predetermined level, usually 5% of the feed concentration. Note that a fraction of the bed is not fully used for adsorption since the feed step was stopped before the bed was fully saturated.

According to Wankat (2007), it is difficult to measure what is happening inside the bed. However, if a column is run to saturation and the outlet concentration is measured, it can infer what happened inside the bed. The outlet concentration profile is shown schematically in Figure 2.2B. The width of the MTZ t_{MTZ} (which is again arbitrarily measured from $0.05c_F$ to $0.95c_F$) is now easy to measure. The length of MTZ inside the bed L_{MTZ} can be calculated as,

$$L_{MTZ} = u_{sh}\, t_{MTZ} \tag{2.1}$$

The shock wave velocity can be calculated from experimental data.

$$u_{sh} = L/t_{center} \tag{2.2}$$

where t_{center} is the time the center of the pattern, $0.5\ (c_F - c_{initial})$, exits the column.
All of the bed up to the MTZ is fully utilized for adsorption. Within the MTZ the fraction of the bed not used is (Area unused bed in MTZ)/(Total area of MTZ). This ratio can be determined from Figure 2.2A or from the measurements shown in Figure 2.2B. Thus, the fraction of used bed is

$$Frac.\ bed\ use = 1 - \left(\frac{Area\ unused\ in\ MTZ}{Total\ Area\ in\ MTZ}\right)\frac{L_{MTZ}}{L} \tag{2.3}$$

Measuring the ratio of the areas isn't necessary if the adsorption system produces a symmetric breakthrough curve (e.g., as shown in Figure 2.2B). For symmetric breakthrough curves the ratio of areas is always one half. Hence, the fraction of the bed use is

$$\text{Frac. bed use} = 1 - 0.5\, L_{MTZ}/L \tag{2.4}$$

For symmetric breakthrough curves if L/L_{MTZ} = 1.0, frac bed use = 0.5; if L/L_{MTZ} = 2.0, frac bed use = 0.75; if L/L_{MTZ} = 3.0, frac bed use = 0.833; if L/L_{MTZ} = 4.0, frac bed use = 0.875, and so forth. The optimal bed length for adsorption is often between two to three times the L_{MTZ}. If a frac bed use is chosen, the column length can be determined.

$$L = 0.5\ L_{MTZ}/(1\text{-frac bed use}) \qquad (2.5)$$

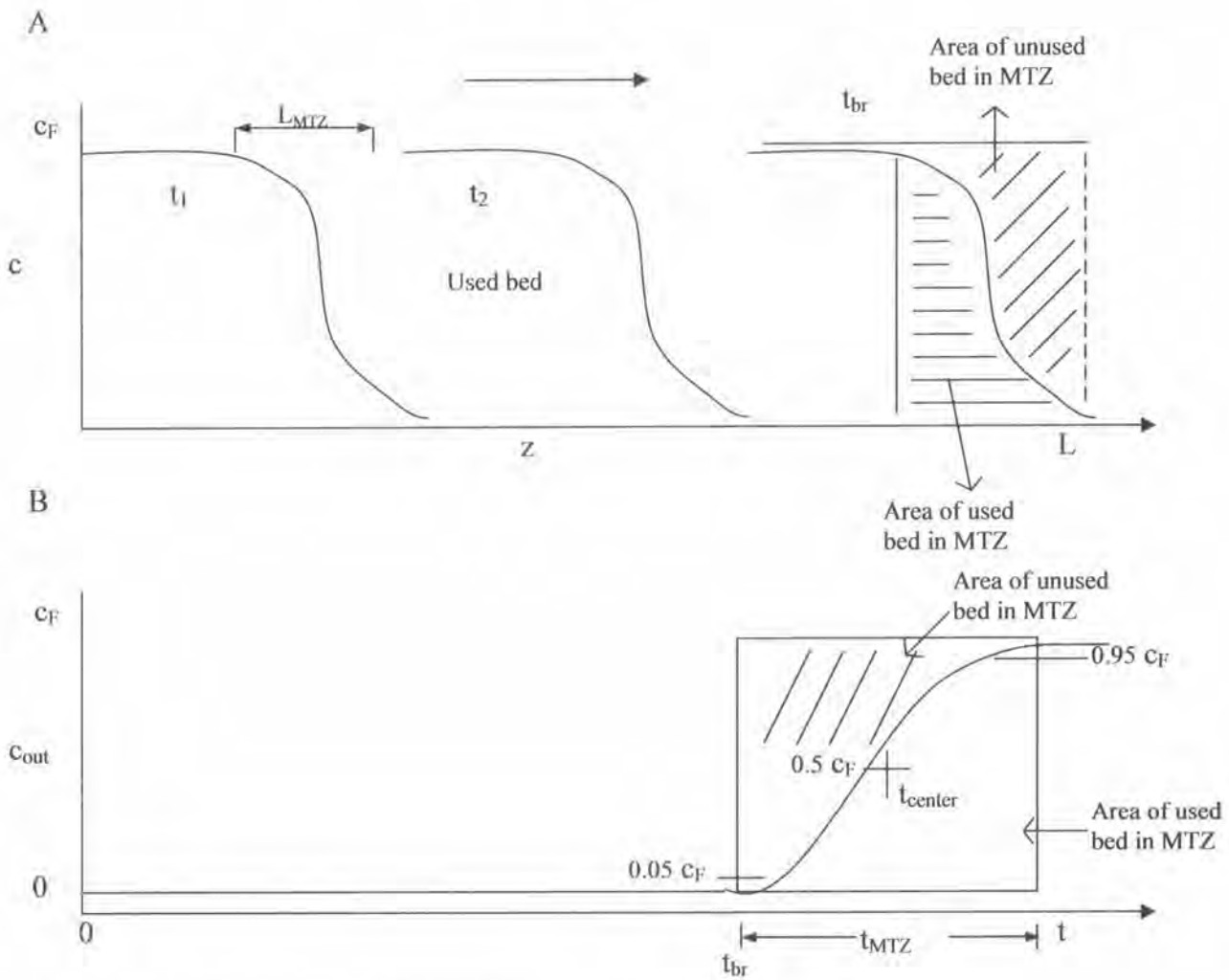

Figure 2.2 The constant pattern wave inside the bed (Wankat, 2007).

Once the frac bed use is known, the bed capacity can be found.

$$\text{Bed Capacity} = (\text{Frac bed use})(\text{Mass or Volume adsorbent})(q_F)$$

where q_F is the amount adsorbed at the feed concentration in the appropriate units. Of course, q_F can be determined from the equilibrium isotherm for an isothermal adsorber or from the experimentally determined value of u_{sh}.

The pattern velocity u_{sh} and the width of the MTZ t_{MTZ} are often measured experimentally with a laboratory column. This measurement needs to be done with the design values for the initial and final concentrations. It is most convenient if the measurement is done with the same velocity and same particle size as in the large-scale unit. However, if pore diffusion controls, the results can be adjusted for changes in velocity and particle diameter. For constant pattern systems the width of the MTZ t_{MTZ} is inversely proportional to $k_{m,q}a_p$.

$$t_{MTZ} \propto \frac{1}{k_{m,q} a_p} \tag{2.6}$$

If pore diffusion controls $k_{m,q}a_p$ can be estimated. The result is,

$$t_{MTZ} \propto \frac{d_p^2}{D_{eff}}, \text{ independent of } v_{inter} \tag{2.7}$$

In ideal fixed-bed adsorption, Seader and Henley (1998) suggest that equilibrium between the fluid and the adsorbent is achieved instantaneously resulting as in a shock like wave, called a stoichiometric front, that moves as a sharp concentration front through the bed if (1) external and internal mass-transfer resistances are very small; (2) plug flow is achieved; (3) axial dispersion is negligible; (4) the adsorbent is initially free of adsorbate; and (5) the adsorption isotherm begins at the origin. Upstream of the front, the adsorbent is saturated with adsorbate and the concentration of solute in the fluid is that of the feed, c_F. The loading of adsorbate on the adsorbent is the q_F in equilibrium with c_F. The length of the bed section upstream of the front is LES, where ES refers to the equilibrium section, called equilibrium zone.

In the upstream region, the adsorbent is spent. Downstream of the stoichiometric front and in the exit fluid, the concentration of the solute in the fluid is zero, and the adsorbent is still adsorbate-free. In this section of the bed, the length is LUB where UB refers to unused bed. For ideal fixed-bed adsorption, the location of

the concentration wave front L as a function of time is obtained solely by material balance and adsorption equilibrium considerations. Accordingly:

$$Q_F c_F t_{ideal} = (q_{ref} S) \tag{2.8}$$

$$Q_F c_F t_{ideal} = q_{ref} (\rho_B V_B) \tag{2.9}$$

$$Q_F c_F t_{ideal} = q_{ref} \rho_B \frac{\pi D^2}{4} (LES) \tag{2.10}$$

$$LES = \left(\frac{Q_F c_F t_{ideal}}{q_{ref} \rho_B \frac{\pi D^2}{4}} \right) \tag{2.11}$$

where Q_F is the volumetric flow rate of feed, c_F is the concentration of the solute in the feed, t_{ideal} is time to breakthrough, q_{ref} is the loading per unit mass of adsorbent that is in equilibrium with the feed concentration, S is the total mass of adsorbent in the bed, ρ_B is the density of the bed, V_B is bed volume, and L_B is the total bed length.

Since the total bed length is know, LUB can be found from:

$$LUB = L_B - LES \tag{2.12}$$

However, when an MTZ is present, then an LUB is necessary and is referred to as the equivalent length of unused bed. To determine LUB from an experimental breakthrough curve, the front is located such that in Figure 2.3, area A is equal to area B. Then:

$$LUB = L_B \frac{t_S - t_b}{t_S} \tag{2.13}$$

where L_B is the length of the experimental bed, t_s is time of the front that makes area A equal to area B, and t_b is breakthrough time.

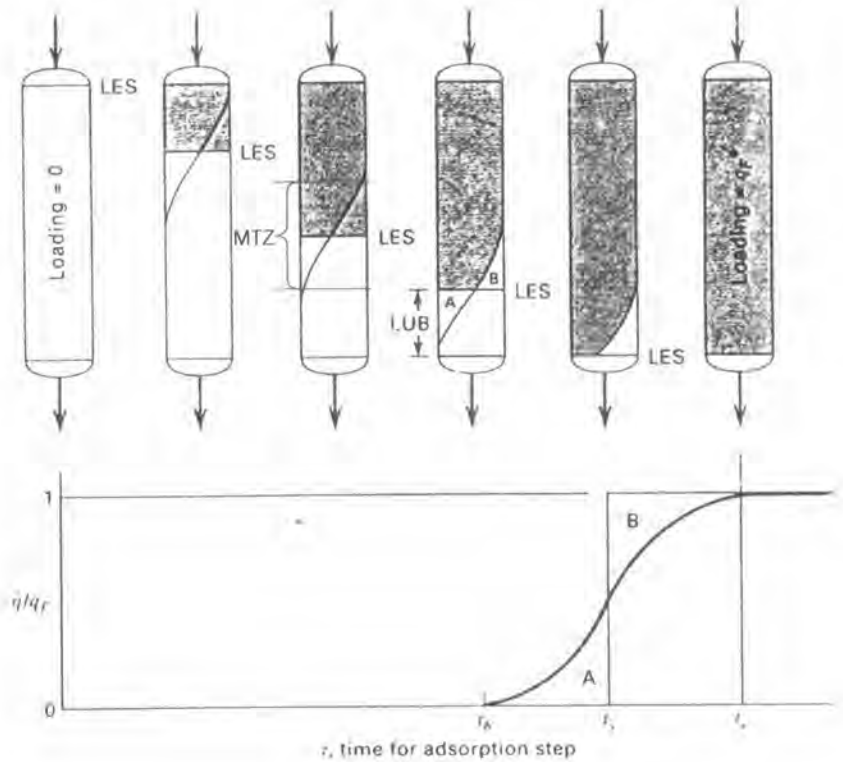

Figure 2.3 Determination of bed length from laboratory measurements (Seader and Henley, 1998).

2.6.2 Adsorbent support and flow distribution

Adsorbent particles can be supported in one or two ways in an adsorption column. The first comprises a series of grids with each successively higher layer having a finer mesh. The second comprises a graded system of inert particles which may range from ceramic balls down in size to gravel. For those applications where the adsorbent may have to be removed from the bottom outlet there may be no support system but the flow distributors may, as a result, be complex.

As suggested by Crittenden and Thomas (1998), at the top of a bed a layer of inert support balls may be used as ballast in order to prevent movement and hence attrition of the adsorbent. The ballast needs to be denser and significantly larger than the adsorbent particles and a retention screen is normally placed on top in order to prevent the ballast from migrating downwards through the bed. The retention screen cannot be settlement in cyclic processes. For gas phase applications in which frequent changes of bed pressure and flow direction occur it is generally necessary to use a pre-load on the top of the adsorbent bed. This pre-load, which might take the form of

a spring or compressed fiber pad, is used to prevent movement and automatically allows for settlement.

Immediate bed supports might be required when the adsorbent is susceptible to damage by crushing. Intermediate bed supports might also be used in compound adsorbent systems in which it may be necessary periodically to change individual adsorbent materials.

Poor fluid flow distribution can be avoided by using a variety of techniques. First, sufficient plenum space should be allowed above and below the fixed bed. Secondly, baffle plates should be fitted when symmetrically placed inlet and outlet are used. The baffle plates, which may be solid, slotted or redirected, its momentum is broken and it cannot impinge directly on the adsorbent particles. If balls or gravels are used to further aid distribution then screens should be used to surround the baffles. Thirdly, it may be necessary to use nozzle headers in which flow can enter the bed from several nozzles along a distribution system. The holes along such a distribution system may not necessarily be of uniform size.

2.6.3 Flow direction

Fixed bed adsorbers commonly are vertical and cylindrical vessels. While horizontal vessels are occasionally used, vertical orientation is preferred to avoid creation of flow maldistribution when settling of a bed or movement of particles within it occurs. Flow can be arranged vertically through a cylindrical vessel which is lying horizontally. In some applications, notably cyclic processes which have many changes of pressure and flow direction, a pre-load is placed on the top of the adsorbent bed to keep the adsorbent particles restrained. If flow is required to be horizontal through a bed lying horizontally then it is likely that flow redistributors will be needed inside the bed to ensure that flow cannot preferentially take place along the top of the vessel once settlement has occurred.

The flow direction for adsorption in a vertical fixed bed is determined not only by the potential for lifting or fluidizing the bed but also by whether the feed is a gas or a liquid. For gas and vapor phase applications velocities which cause crushing of an

adsorbent tend to be much higher than those required to lift a bed and therefore it is convenient to arrange to have the highest flowrate in the downwards direction through a vertical bed.

For liquid phase applications the buoyancy forces need to be considered as well. The flow velocity in the upwards direction should normally be sufficiently low to prevent bed lifting. However, in some applications it is desirable to allow some bed expansion to occur and so limit the pressure drop. As the minimum velocity to cause lifting is exceeded, the pressure drop increases only slightly with further increases in velocity. Too much expansion, however, can cause the bed to become well mixed. If this were to occur within a fixed bed then it would resemble the batch process and create the risk of reduced purity in the product. Other problems caused by high velocities include abrasion, attrition and erosion. When desirable, expansion is accordingly limited normally to about 10%.

2.7 Design of fixed-bed adsorption columns

Two macroscopic methods to design adsorption columns are the scale-up and kinetic approaches. Both methods rely on breakthrough data obtained from pilot columns. The scale-up method is very simple, but the kinetic method takes into account the rate of adsorption (determined by the kinetics of surface diffusion to the inside of the adsorbent pore). The scale-up approach is useful for determining the breakthrough time and volume (time elapsed and volume treated before the maximum allowable effluent concentration is achieved) of an existing column, while the kinetic approach will determine the size requirements of a column based on a known breakthrough volume.

2.7.1 Scale-up approach

Initially, a pilot column with a bed volume (V_p) and volumetric flow rate of fluid (Q_p) is used. As shown in Figure 2.4, the total volume (V_T^{pilot}) of the fluid that passes through the column is measure until the outlet solute concentration is observed to rise to the maximum allowable value (C_a).

The (plant-scale) design column should operate such that:

1. Fluid residence time in the pilot and design column are the same.
2. The total volume of fluid processed until breakthrough per mass of adsorbent in the column is the same for both columns.

The parameters need to effect the scale-up are:

$(BV) = (V_p)\ Q/Q_p$ = Bed volume of design column, where Q is the fluid volumetric flow rate of the design column

$M = (BV)(\rho_s)$ = mass of adsorbent in the design column (ρ_s = adsorbent bulk density)

V_T^{pilot} = breakthrough volume of the pilot column (chosen to correspond to the maximum allowable effluent solute concentration). This volume is the total amount treated before breakthrough occurs in the pilot column.

$\hat{V}_B = \frac{V_T^{pilot}}{M^{pilot}}$ = volume of liquid treated per unit mass of adsorbent (same for both columns)

$M_t = Q/\hat{V}_T$ = mass of adsorbent exhausted per hour in design column Q.

$t_{bt} = M/M_t$ = breakthrough time for the design column

$V_T = Q\ t_{bt}$ = breakthrough volume for the design column

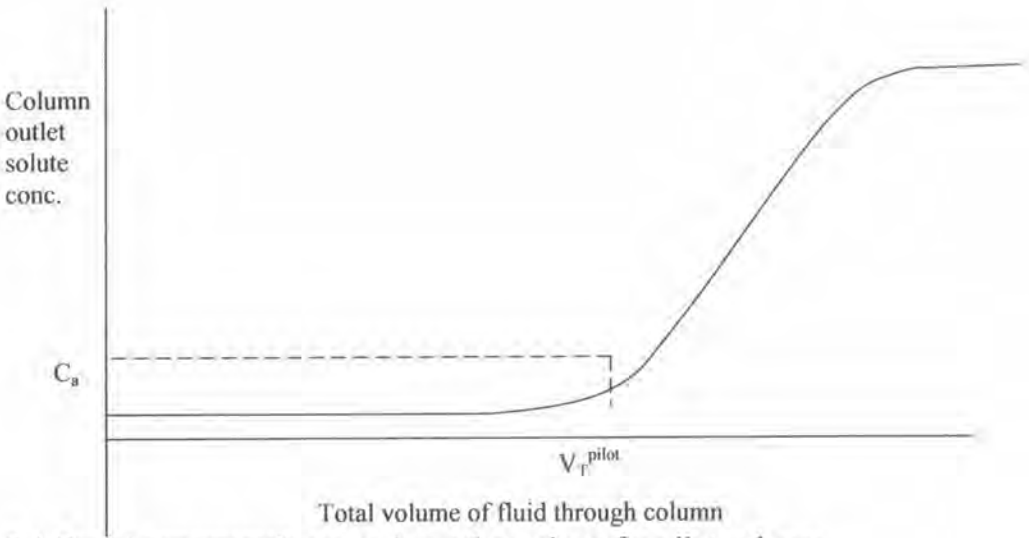

Figure 2.4 Outlet concentration vs volume throughput for pilot column.

2.7.2 Kinetic approach

If the design fluid volumetric flow rate (Q) is sufficiently low that equilibrium is rapid in comparison, the Equation 2.14 below is a good approximation of the concentration profile for the breakthrough curve as a function of fluid volume (V) put through the column. A Langmuir isotherm is assumed where k_1 is the adsorption rate constant for this isotherm. When $q_0M >> C_0V$, the effluent solute concentration is approximately zero. For $q_0M << C_0V$, the effluent solute concentration is C.

$$\frac{C}{C_0} \cong \frac{1}{1+\exp\left[\frac{k_1}{Q}(q_0M - C_0V)\right]} \qquad (2.14)$$

Where C = effluent solute concentration

C_0 = influent solute concentration

k_1 = rate constant

q_0 = maximum solid-phase concentration of the sorbed solute (g/g or lb/lb)

M = mass of the adsorbent

V = throughput volume

Q = fluid volumetric flowrate.

The equation can be rewritten as:

$$\ln\left(\frac{C}{C_0}-1\right)=\frac{k_1 q_0 M}{Q}-\frac{k_1 C_0 V}{Q} \qquad (2.15)$$

which is a straight line on a plot of effluent solute concentration vs volume of fluid treated, and the pilot column breakthrough data can be used to determine k_1, q_0, and other parameters of the design column.

2.8 Equilibrium Considerations

In adsorption, a dynamic phase equilibrium is established for the distribution of the solute between the fluid and the solid surface. This equilibrium is usually expressed in terms of (1) concentration (if the fluid is a liquid) or partial pressure (if the fluid is a gas) of the adsorbate in the fluid and (2) solute loading on the adsorbent, expressed as mass, moles, or volume of adsorbate per unit mass of the adsorbent (Seader and Henley, 1998). Unlike vapor-liquid and liquid-liquid equlibria, where theory is often applied to estimate phase distributions, particularly in the form of K-values for the former type of equilibrium, no acceptable theory has been developed to estimate fluid-solid adsorption equlibria. Thus, it is necessary to obtain experimental equilibrium data for a particular solute, or mixture of solutes and/or solvent, and a sample of the actual solid adsorbent material of interest. If the data are taken over a range of fluid concentrations at a constant temperature, a plot of solute loading on the adsorbent versus concentration or partial pressure in the fluid, called an adsorption isotherm, is made. This equilibrium isotherm places a limit on the extent to which a solute is adsorbed from a given fluid mixture on an adsorbent of given chemical composition and geometry for a given set of conditions. The rate at which the solute is adsorbed is also an important consideration and is discussed in the next section.

2.8.1 Freundlich Isotherm

The equation attributed to Freundlich is empirical and nonlinear in pressure.

$$q = kp^{1/n} \qquad (2.16)$$

where k and n are temperature-dependent constants. Generally, n lies in the range of 1 to 5. With n = 1, Equation 2.16 reduces to Henry's law equation which is called the **linear isotherm**. Experimental q-p isothermal data can be fitted to Equation 2.16 by a nonlinear curve-fitting computer program or by converting Equation 2.16 to a linear form as follows, and using a graphical method or a linear regression program:

$$\log q = \log k + (1/n) \log p \qquad (2.17)$$

If the graphical method is employed, the data are plotted as log q versus log p. The best straight line through the data has a slope of (1/n) and an intercept of log k. In general, k decreases with increasing temperature, while n increases with increasing temperature and approaches a value of 1 at high temperatures. Equation 2.17 is derived by assuming a heterogeneous surface with a nonuniform distribution of the heat of adsorption over the surface.

2.8.2 Langmuir Isotherm

The Langmuir equation is derived form simple mass-action kinetics, assuming chemisorption. Assume that the surface of the pores of the adsorbent is homogeneous (ΔH_{ads} = constant) and that the forces of interaction between adsorbed molecules are negligible. Let θ be the fraction of the surface covered by adsorbed molecules. Therefore, $(1- \theta)$ is the fraction of the bare surface. Then, the net rate of adsorption is the difference between the rates of adsorption and desorption:

$$dq/dt = k_a p(1- \theta) - k_d \theta \qquad (2.18)$$

At equilibrium, $dq/dt = 0$ and (2.18) reduces to

$$\theta = \frac{K_p}{1 + K_p} \tag{2.19}$$

where K is the adsorption equilibrium constant (= k_a/k_d). Here,

$$\theta = q/q_m \tag{2.20}$$

where q_m is maximum loading corresponding to complete coverage of the surface by the gas. Thus, the Langmuir adsorption is restricted to a monomolecular layer. Combining (2.20) with (2.19), following can be obtained:

$$q = \frac{Kq_m p}{1 + Kp} \tag{2.21}$$

At low pressure, if Kp << 1, (2.21) reduces to the linear Henry's law form, while at high pressure where Kp >>1, q = q_m. At intermediate pressure, (2.21) is nonlinear in pressure. Although originally devised by Langmuir for chemisorption, (2.21) has been widely applied to physical adsorption data.

The quantities K and q_m in (2.21) are treated as empirical constants, obtained by fitting the nonlinear equation directly to the experimental data or by employing the following linearized from, numerically or graphically:

$$\frac{p}{q} = \frac{1}{q_m K} + \frac{p}{q_m} \tag{2.22}$$

Using (2.22), the best straight line is drawn through a plot of points p/q versus p, giving a slope of ($1/q_m$) and an intercept of $1/(q_m K)$. If the theory is reasonable, K should change rapidly with temperature, but q_m should not because it is related through υ_m (volume of monomolecular layer of gas adsorbed at STP) to the specific surface area of the adsorbent, S_g. It should be noted that the Langmuir isotherm predicts an asymptotic limit for q at high pressure, whereas the Freundlich isotherm does not.

2.9 Transport processes

Adsorption is typically operated as an equilibrium-limited process; the adsorbent must be in equilibrium with the surrounding fluid phase to obtain maximum adsorption. It is also important to consider the various transport processes involved and the rate at which adsorption will occur. The mass transfer mechanism of adsorption typically has four steps (Figure 2.5).

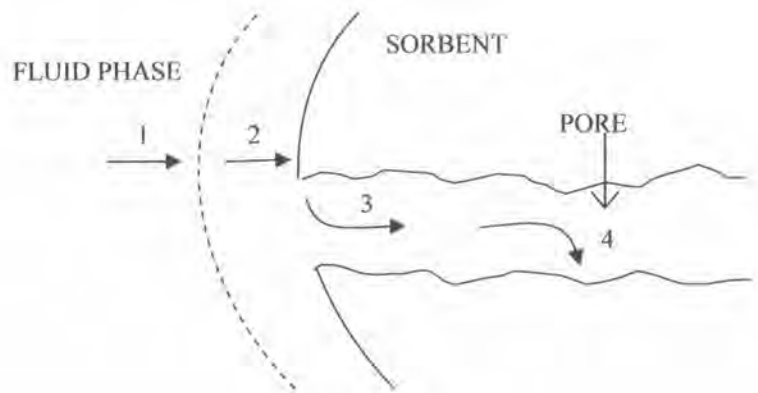

Figure 2.5 Adsorption mechanisms.

1. Transfer of the solute (adsorbate) from the bulk fluid phase to the surface film (boundary layer) which surrounds the adsorbent particle. This step is controlled by convective flow and turbulent mixing.

2. Transfer of the adsorbate across the surface film to the exterior surface of the adsorbent particle. This step is controlled by molecular diffusion and/or convective flow.

3. Transfer of the adsorbate from the particle surface to the interior of the adsorbent via the pore network. This step can be accomplished in two ways: pore diffusion (diffusion through the fluid in the pore); and surface diffusion (the particle travels along the pore surface).

4. Physical or chemical binding or the adsorbate to the internal surface of the adsorbent. This step is controlled by the molecular interactions described previously for adsorption.

Steps 1 and 4 are usually the fastest steps, and therefore are not considered to contribute to the overall rate of adsorption. The rate-determining step is typically Step 3, although changes in fluid flow rates can affect mass transfer across the fluid-particle boundary layer (Step 2).

For fixed beds, Step 2 can be described by:

$$j = 1.17\ \mathrm{Re}^{-0.415} \qquad 10 < \mathrm{Re} < 2500 \qquad (2.23)$$

$$= \frac{k}{\upsilon_s} Sc^{0.067} = \text{Chilton-Colburn } j \text{ factor} \qquad (2.24)$$

Where $\mathrm{Re} = \dfrac{\rho \upsilon_s d_p}{\mu}$ = Reynolds number

$Sc = \dfrac{\mu}{\rho D_{AB}}$ = Schmidt number

ρ_f = fluid density

μ = fluid viscosity

υ_s = fluid superficial velocity

d_p = particle diameter

k = mass transfer coefficient

D_{AB} = diffusion coefficient of sorbate in fluid

High values of k correspond to less mass transfer resistance for this step. One way to increase k is to increase υ_s. This can cause problems, though, since the contact time in the bed would be reduced. This can lead to breakthrough with a larger portion of the bed unused.

A better alternative is a low value of υ_s. This approach provides more contact time for sorbate-sorbent equilibrium and a lower pressure drop across the bed. In

practice, this translates to the use of short bed lengths of large diameter (low υ_s), in contrast to long, small-diameter beds (high υ_s). The pressure drop across the bed can be estimated using the Ergun equation:

$$\frac{\Delta P}{L}=\left(150\frac{1-\varepsilon}{\mathrm{Re}}+1.75\right)\frac{\rho_f \upsilon_s^3(1-\varepsilon)}{d_p\varepsilon^3} \qquad (2.25)$$

where L = actual bed length

ε = bed void fraction (not particle).

Remember that the total pressure drop includes accounting for auxiliary components (valves, piping, etc). Step 3 depends on the adsorbent size and the effective diffusivity (D_{eff}) within the adsorbent particle, which can be written as

$$D_{eff}=\frac{D_{AB}\varepsilon_p}{\tau} \qquad (2.26)$$

where ε_p = particle void fraction

τ = tortuousity (correction factor > 1 to account for the tortuous nature of pore structure).

2.10 Non-isothermal effects

Many adsorption design approaches assume that adsorption is occurring isothermally. This is a good assumption only when the adsorption component concentration is low and/or the heat of adsorption is low. There are two simple methods that can be used to determine if the system can be assumed to be isothermal. Since most of the heat is generated in MTZ where adsorption is occurring, the rate at which the heat can be transferred out of this zone compared to the movement of the MTZ is the basis for one method. This comparison is shown by the "crossover ratio" R:

$$R = \frac{C_{pf}(X_i - X_{res})}{C_{ps}(Y_i - Y_o)} \tag{2.27}$$

where Y is the molar ratio of sorbate to the carrier fluid (i denotes inlet, o denotes outlet), and the fluid and sorbent heat capacities, C_{pf} and C_{ps}, include the effect of the sorbate. X is the sorbent loading (wt sorbate/wt sorbent); X_{res} is the residual loading in the bed prior to the adsorption step. When $R >> 1$, the heat is easily removed from the MTZ and adsorption can be assumed to be isothermal. As R approaches a value of 1, more and more heat will be retained in the MTZ. An increase in the temperature of the "leading" or breakthrough end of the MTZ will lower the equilibrium loading from the isothermal value based on the inlet temperature and cause the curve to become less favorable relative to the operating line, until ultimately the MTZ has no stable limit but continues to expand as it moves through the bed. When $R = 1$, the heat front is moving through the bed at the same velocity as that of the MTZ, and essentially all the heat of adsorption is found in the MTZ. For cases where $R < 1$, the heat front will lag the adsorption front and heat will be stored in the equilibrium section. Here the temperature rise will cause the equilibrium loading to decrease. Thus, the crossover ratio is an indication of non-isothermal operation, the extent of the harmful effects of the temperature rise due to adsorption, and the location of the temperature change.

A second method computes the temperature rise under equilibrium condition

$$\Delta T = T_{max} - T_f = \frac{q\Delta H / C_{pg}}{(q/Y)_f - C_{ps}/C_{pg}} \qquad (2.28)$$

where q = solute adsorbed/mass of sorbent

ΔH = heat of adsorption

Y = mass solute in fluid phase/mass of carrier gas

C_p = heat capacity,

And the subscript are:

s = sorbent

g = gas

f = feed.

For many operating conditions $C_{ps}/C_{pg} << (q/Y)_f$, so the above equation reduces to

$$\Delta T = Y_f \Delta H / C_{pg}. \qquad (2.29)$$

A quick estimate of ΔT for gas-phase sorption can be made. ΔH has a range of 1000 to 4000 kJ/kg (avg = 2500), C_{pg} is approximately 1 kJ/kg.K and Y_f is typically 0.01. Therefore:

$$\Delta T = \frac{\left(0.01 \frac{kg\ solute}{kg\ carrier\ gas}\right)\left(2500 \frac{kJ}{kg\ solute}\right)}{1 \frac{kJ}{kg\ carriergas.K}} = 25\,K\ (\equiv 25°C)$$

So the maximum temperature rise in a gas-solid sorption can reach 25 °C.

A few additional points are worth noting:

1. For constant partial pressure, Y_f is inversely proportional to total pressure. Therefore, ΔT will decrease with an increase in total pressure. This translates to isothermal operation for a total feed pressure of approximately 50 atm.

2. Carrier gasses with high C_{pg} (hydrogen, for example) will tend to reduce ΔT.

3. An increase in feed solute concentration will increase ΔT.

2.11 Pressure Swing Adsorption prediction

The most common contacting device for adsorption, chromatography, and ion exchange is the packed bed shown schematically in Figure 2.6. The particles are packed in the cylindrical column of cross-sectional area A_c and the length of packed section is L. Some type of support netting or frit is used at the bottom of the packed section and hold down device such as a net or frit is used at the top of the packed section. Figure 2.6 demonstrates a number of important variables. The external porosity ε_e is the fraction of the column volume that is outside the particles. To some extent the value of ε_e depends on the shape of the particles (e.g. ε_e is smaller for spheres than for irregular shaped particles) and the packing procedure used. It is important to have a uniformly packed column with a constant value of ε_e. The internal porosity ε_p is the fraction of the volume of the pellets that consists of pores and thus, is available to the fluid. The total volume available to the fluid is

$$V_{fluid} = [\varepsilon_e + (1 - \varepsilon_e)\,\varepsilon_p]\, V_{column} \qquad (2.30a)$$

From this equation we can define the total porosity ε_e as the sum of all the voids.

$$\varepsilon_T = \varepsilon_e + (1 - \varepsilon_e)\,\varepsilon_p \qquad (2.30b)$$

Porosities are dimensionless quantities.

Although the fluid can fit into all the pores, molecules such as proteins may be too big to fit into some or all of the pores. This size exclusion can be quantified in terms of a dimensionless parameter K_d where $K_d = 1.0$ if the molecule can penetrate all of the pores and $K_d = 0$ if the molecule can penetrate none of the pores. The value of $K_{d,i}$ for a given molecule i can also be between 0 and 1 since the pores are not of uniform size. The volume available to a molecule is,

$$V_{available} = [\varepsilon_e + (1 - \varepsilon_e)\,\varepsilon_p\,K_{d,i}]\,V_{column} \qquad (2.30c)$$

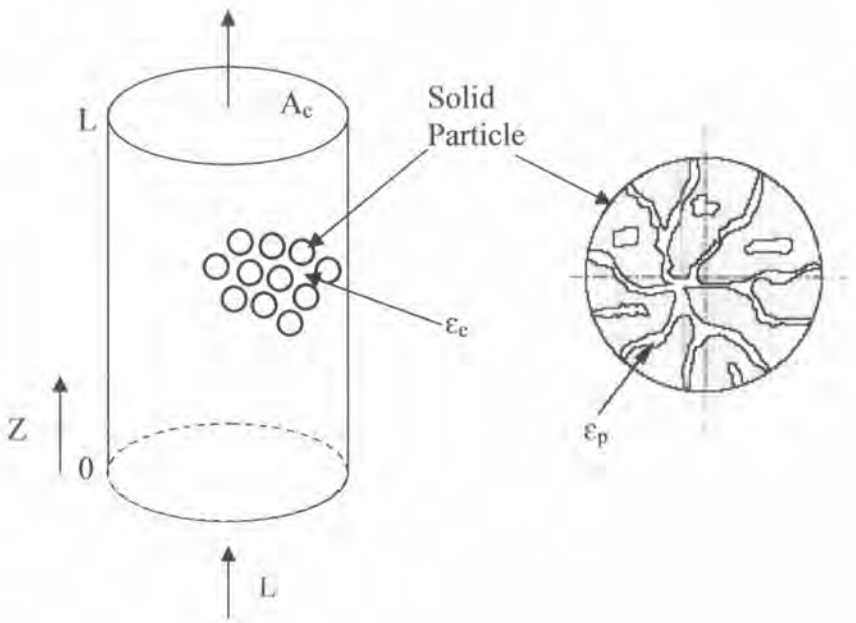

Figure 2.6 Schematic of adsorption and particle (Wankat, 2007).

This picture is useful but does not match all adsorbents. Gel type ion-exchange resins have no permanent pores. Instead they consist of a tangled network of interconnected polymer chains into which the solvent dissolves. In effect, $\varepsilon_p = 0$. Macroporous ion-exchange resins have permanent pores and $\varepsilon_p > 0$, but often $K_d < 1.0$ for large molecules. Many activated carbons have both macropores and micropores; thus, there are two internal porosities. Molecular sieve zeolite adsorbents are used as pellets that are agglomerates of zeolite crystals and a binder such as clay. In this case, there is an interpellet porosity (typically, ε_e ~0.32), and intercrystal porosity (ε_{p1} ~0.23), and an intracrystal porosity (ε_{p2} ~0.19), which has $K_{d,i} \leq 1.0$.

Two different velocities are typically defined for the column shown in Figure 2.6. The superficial velocity, which is easy to measure, is the average velocity the volumetric flow of fluid would have in an empty column. Thus,

$$v_{super} = Q / A_c \qquad (2.31a)$$

where Q is the volumetric flow rate (e.g., in m^3/s), the cross sectional area $A_c = D^2_{col}/4$ is in m^2 and v_{super} is in m/s. The interstitial velocity v_{inter} (also in m/s) is the average velocity the fluid has flowing in between the particles. Since the cross sectional area actually available to the fluid is $\varepsilon_e A_c$, a mass balance in the flowing fluid is

$$v_{inter}\, \varepsilon_e\, A_c = v_{super}\, A_c$$

$$v_{inter} = v_{super} / \varepsilon_e \qquad (2.31b)$$

Since ε_e is less than 1.0, $v_{inter} > v_{super}$. Very large molecules that are totally excluded from the pores and are not adsorbed move at an average velocity of v_{inter}.

There are also different densities of interest. The first, the fluid density ρ_f (e.g., in kg/m^3) is familiar. The second density is the structural density ρ_s (e.g., also in kg/m^3) of the solid. This is the density of the solid if it is crushed and compressed so that there are no pores and all of the air is removed. The particle or pellet density ρ_p is the average density of the particles consisting of solid plus the fluid in the pores.

$$\rho_p = (1-\varepsilon_p)\,\rho_s + \varepsilon_p\,\rho_f \qquad (2.32a)$$

Manufacturers often report a bulk density ρ_b of the adsorbent. This density is the weight of the adsorbent as delivered, which includes fluid in the pores and between the particles, divided by the volume of the container. The bulk density can be calculated from the other densities.

$$\rho_b = (1-\varepsilon_e)\,\rho_p + \varepsilon_e\,\rho_f \qquad (2.32b)$$

The bulk and particle densities will also be in kg/m3. If the fluid is a gas with $\rho_f << \rho_b$,

$$\rho_b = (1-\varepsilon_e)\,\rho_p = (1-\varepsilon_e)\,(1-\varepsilon_p)\,\rho_s \text{ (when fluid is gas)} \qquad (2.32c)$$

Pressure swing adsorption (PSA) and vacuum swing adsorption (VSA) cycles are alternatives to thermal cycles for gas systems. They are particularly useful for more concentrated feeds and adsorbates that are not strongly adsorbed. Figure 2.7A shows the steps in the basic Skarstrom cycle for PSA. Usually, the desired product is the pure product gas after adsorbate removal. Typical applications include drying gases, purifying hydrogen, and reproducing oxygen or nitrogen from air.

Following the feed step at the higher pressure, the pressure in the column is reduced to the lower pressure by counterflow blowdown. At this reduced pressure the column is purged (counterflow to the feed) using part of the pure product gas. Since pure product gas is used as a purge, the purge product (or waste) gas contains both adsorbate and carrier gas. The volume of purge gas required for the Skarstrom cycle is,

$$V_{purge} = \gamma V_{feed} \qquad (2.33)$$

where γ typically is between 1.15 and 1.5. Because of the volumetric expansion of the product gas from p_h to purge gas at p_L, significantly less moles of purge gas are needed than feed gas. Dropping the pressure also reduces the partial pressure, which helps desorb the adsorbate. The final step in the Skarstrom cycle is repressurization of the column. This step was originally done with fresh feed gas although with concentrated systems it is now much more common to use high-pressure product gas as shown in Figure 2.7. Usually two or more columns are operated in parallel, but with cycles out of phase so that one column is producing product when the other needs to be purged or repressurized. One method of doing this is shown in Figure 2.7B systems with from one to twelve columns are used commercially. PSA has the advantage that cycles can be very fast – a minute or two is common in industry and come cycles are as short as a few seconds. These short cycles lead to high productivity and hence relatively small adsorbers.

Figure 2.8 illustrates a simple vacuum swing cycle. The feed enters at the high pressure, which may be essentially atmospheric pressure. If p_h is significantly above atmospheric pressure, a short optional blowdown step is included. Then a vacuum pump is used to reduce the pressure to very low pressures. At very low pressures the partial pressure is very low and very little adsorbate can be adsorbed (see Figure 2.8). Unfortunately, this step is slow and productivities of VSA systems are low. However, VSA has the advantage that a relatively pure product gas and a relatively pure adsorbate product can be produced. For example, VSA units can separate air into an oxygen product and a nitrogen product. The final step is repressurization of the column. VSA units are usually operated with several columns in parallel. A large number of variations of PSA, VSA, and combinations of PSA and VSA cycles have been invented (Kumar, 1996; Ruthven *et al.*, 1994; Tondeur and Wankat, 1985). For

example, the purge step in a PSA cycle may be operated at a pressure less than atmospheric pressure.

The simple Skarstrom cycle for PSA shown in Figure 2.7A has constant pressure (isobaric) periods and periods when pressure is changing. It is assumed that a very dilute gas stream containing trace amounts of asdorbate A in an weakly adsorbed carrier gas is being accurate. If mass transfer is very rapid, then the solute movement theory can be applied. Since the system is very dilute, the gas velocity is constant and the system is assumed to be isothermal. In more concentrated PSA systems neither of these assumptions is true, and a more complicated theory must be used.

During the isobaric periods (feed at p_h and purge at p_L) the solute moves at a velocity u_s. For a gas that can be assumed to be ideal and an isotherm in partial pressure units, the solute velocity is given by Equation 2.34. Normally, $K_{d,i} = 1.0$ and all of the adsorption sites are accessible to the small gas molecules.

$$u_{s,i} = \frac{v_{interstitial}}{1 + \frac{(1-\varepsilon_c)\varepsilon_p K_{d,i}}{\varepsilon_c} + \frac{(1-\varepsilon_c)(1-\varepsilon_p)}{\varepsilon_c}\rho_s RTK'_{A,p}} \qquad (2.34)$$

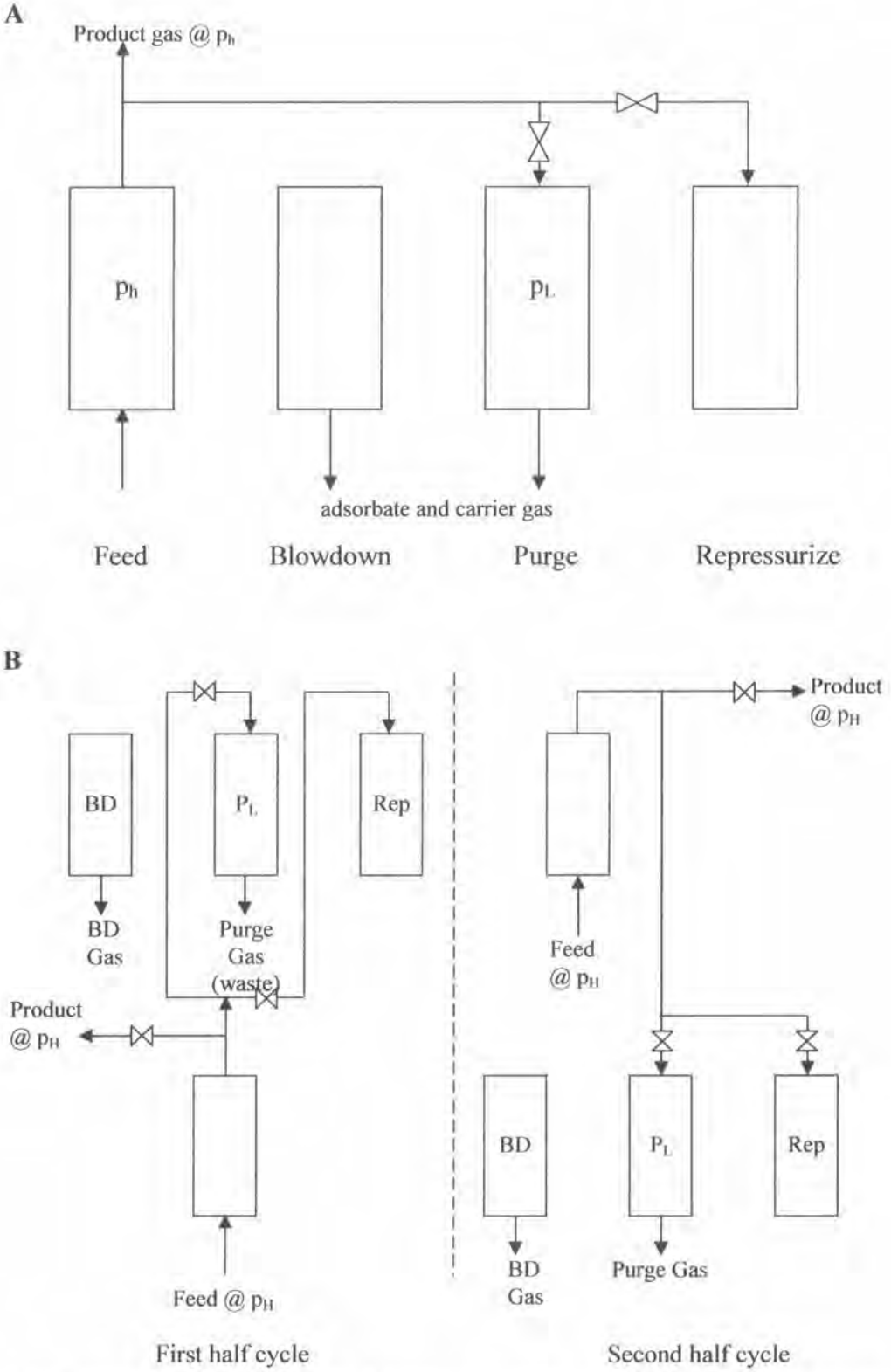

Figure 2.7 Pressure swing adsorption; A) steps for single column in Skarstrom cycle, B) use of two columns in parallel for continuous feed and product. Period of feed step = period of blowdown + purge + repressurization steps.

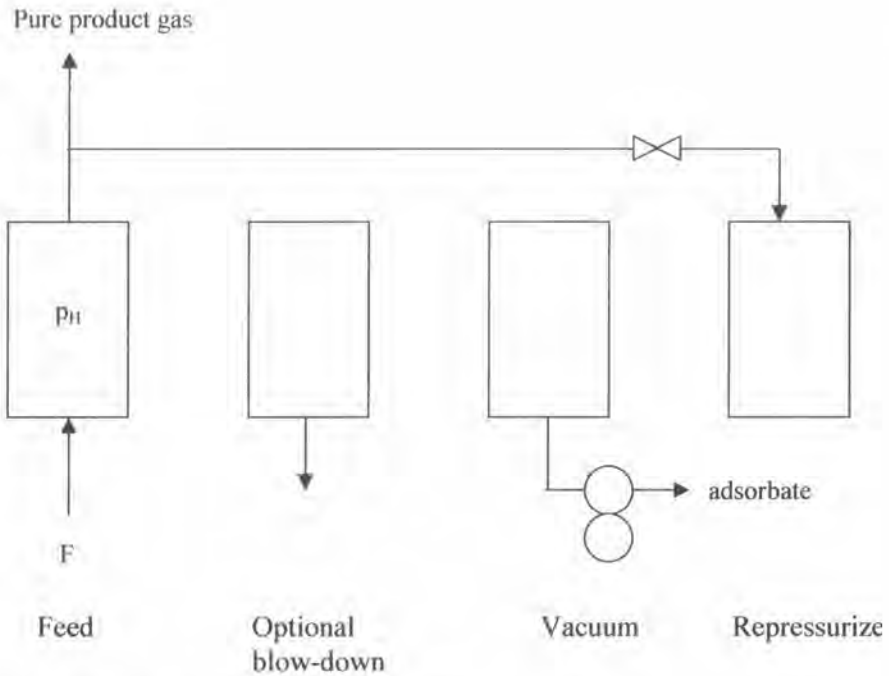

Figure 2.8 Basic vacuum swing adsorption cycle.

During blowdown the mole fraction of adsorbate in the gas increases because of desorption as the pressure drops. During repressurization the opposite occurs and the adsorbate mole fraction in the gas decreases. When the pressure changes, the solute waves also shift location. Determining the mole fraction changes and shifts in location for these steps requires solution of the partial differential equations for the system. The results for linear isotherms are relatively simple. Define parameter β_{strong} for the strongly adsorbed component as

$$\beta_{strong} = \frac{\varepsilon_e + (1-\varepsilon_e)\varepsilon_p K_{d,i} + (1-\varepsilon_e)(1-\varepsilon_p)\rho_s K'_{weak} RT}{\varepsilon_e + (1-\varepsilon_e)\varepsilon_p K_{d,i} + (1-\varepsilon_e)(1-\varepsilon_p)\rho_s K'_{strong} RT} = \frac{u_{s,strong}}{u_{s,weak}} \quad (2.35)$$

This parameter measures the ratio of the amount of weakly adsorbed to the amount of strongly adsorbed adsorbate in a segment of the column (Tien, 1994). If the weakly adsorbed component does not adsorb, then $K'_{weak} = 0$ in Equation 2.35. Since $K'_{weak} < K'_{strong}$, $\beta_{strong} < 1.0$. Then the shift in mole fraction of the strongly adsorbed species A is

$$\frac{y_{A,after}}{y_{A,before}} = \left[\frac{p_{after}}{p_{before}}\right]^{\beta_{strong}-1} \quad (2.36)$$

Equation 2.36 predicts an increase in mole fraction y_A for a decrease in pressure. The shift in location of solute waves can be found from

$$\frac{z_{after}}{z_{before}} = \left[\frac{p_{after}}{p_{before}}\right]^{-\beta_{strong}} \tag{2.37}$$

where the axial distance z must be measured from the end of the column that is closed (this can vary during the PSA cycles). Note that if $z_{before} = 0$, then $z_{after} = 0$ also. Solute waves at the closed end of the column cannot shift.

2.12 Literatures Review

Due to its complicated nature and multiple decision parameters including plant dimensionality and operating condition, the design of PSA processes is not a trivial task. Most previous studies on PSA design have been made through rigorous modelling and experimental investigation for specific separation tasks. Meanwhile, the studies of ethanol-water separation have largely been made in a simplified PSA system or a small lab-scale adsorber.

Teo and Ruthven (1986) first studied the adsorption of water from aqueous ethanol using 3A molecular sieves. The adsorptive dehydration of ethanol-water mixture on 3A zeolite was studied experimentally by following the uptake curves for a closed batch system and by measuring breakthrough curves for a packed column. This system was potentially attractive for the dehydration of rectified spirit in the production of fuel ethanol. The equilibrium isotherm was almost rectangular, and the kinetic data for both systems were found to be satisfactorily correlated in terms of simple kinetic models. The results of experiments in which particle size and fluid velocity were varied showed that intraparticle diffusion was the main resistance to mass transfer with some contribution from external film resistance at low fluid velocity and low water concentrations.

Sowerby and Crittenden (1988) compared the recovery by adsorption of ethanol from aqueous vapors of composition around that of the azeotrope in fixed beds packed with various type A molecular sieves. For similar adsorption and desorption conditions, it was proven that 4A was superior to 3A molecular sieve giving higher capacities, shorter mass transfer zone lengths and greater rates of desorption. Very low water concentrations (<0.05 wt% water) could be achieved provided that the initial bed temperature and initial water concentration in the feed were not too high. In addition, it was discovered that type 5A and 10A molecular sieves were not suitable for this separation since high temperature increases which arose from the adsorption of both water and ethanol caused the ethanol to react to form undesirable by-products.

Carmo and Gubulin (2002) carried out an investigation on ethanol-water separation employing a PSA adsorption cycle with zeolite 3A as adsorbent. The cycle was operated in a single fixed bed under various operating adsorption temperature, feed flow, and adsorption pressure. All the experimental runs were performed under vacuum in the desorption step. The effect of these variables on the enrichment and recovery percentage of the product, on the productivity and on the total cycle time was studied, using the adsorption pressure as a parameter. The results of the study concurred with the proposition made by Trent (1993) that these variables significantly affected the responses of interest.

The experiments were organized by a three-level factorial design. The results obtained were compared with the fitted empirical equations as well as with the corresponding surface responses and all variables showed to be influential. Furthermore, an optimal combination of the variables was proposed by means of the ridge analysis method and the optimized multi-response method.

Guan and Hu (2003) studied the numerical simulation of a one column PSA for dehydration of mixture of ethanol and water by the electrical analogue model. The simulation was based on feed pressure of 2.0-5.0 bar, operating temperature of 120-150 °C, and vacuum desorption. It was found that increasing feed pressure may increase recovery and productivity. Furthermore, it was suggested that the use of anisotropic valve connecting the column entrance with the product tank may improve the operating results to obtain 99.9% ethanol and 69% recovery at feed pressure of 2.0 bar and blowdown to 0.4 bar. The study proposed that the PSA system could yield higher recovery and productivity rates if lower product concentration could be accepted.

Sorption of water and ethanol in zeolites 3A and 5A was investigated by Lalik *et al.* (2006) using gas flow-through microcalorimetry in view of finding differences in these materials performance as potential adsorbents in the process of drying of ethanol. In the experiments, both zeolites showed comparable properties for the sorption of water. But they differed profoundly in their sorption of ethanol, which was negligible small in zeolite 3A compared to zeolite 5A, in spite of the much larger enthalpy of adsoption of ethanol in zeolite 3A. The difference was explained in terms

of a steric hindrance preventing the ethanol molecules from entering the narrow pores of the 3A structure, with the 5A structure remaining easily accessible for both the water and ethanol molecules. A size selectivity index, defined as the ratio of sorption capacity of water and ethanol, was proposed to characterize the applicability of a zeolite as sorbent for drying ethanol. It was found that the thermal effect of sorption of water in zeolite 3A was found to be a function of the nature of carrier gas, He or N_2, used in microcalorimetric measurements.

The effect of heat of adsorption on the adsorptive drying of solvents at equilibrium in a packed bed of zeolite was studied by Salem and Shebil (1999). In the experiment a packed bed of 3A zeolite was used to dry ethanol solutions initially at 24 °C and containing up to 6.6 wt.% water. In view of the highly exothermic nature of the process, the progress of the thermal wave through the bed is followed and its effect on product dryness identified. It was stated that the thermal wave was found to leave the bed around the time at which breakthrough of water began to occur. It was also claimed that for a given flow rate, the water concentration in the initial effluent and the peak temperature rise were found to be directly proportionally to the water concentration in the feed.

Meanwhile, for a given feed concentration, it was suggested that both the initial effluent water concentration and the peak temperature rise could be reduced by decreasing the feed velocity. The paper concluded that very low concentrations should be achievable by removing the exotherm. In addition, equilibrium isotherms were reported for the adsorption of water on 3A molecular sieve zeolite and the individual isotherms conform closely to Langmuir and Freundlich models.

Banat *et al.* (2000) investigated the effect of the presence of 3A and 4A molecular sieves on the analysis of vapor-liquid equilibrium (VLE) of ethanol-water system using headspace gas chromatography (HSGC) technique. The VLE of the system was considerably altered in the presence of molecular sieves and the azeotropic point was eliminated. Attractively, in the presence of molecular sieves, pure ethanol was obtained from a feed composition of 40 mol. % ethanol. The separation efficiency was a function of the weight and pore size of molecular sieves.

Moreover, the results obtained in this study added to the validity of using the HSGC apparatus in studying the VLE in various systems.

In addition to the studies of PSA process for ethanol-water separation, Jain *et al.* (2003) attempted to develop easy-to-use rules for PSA process design, based on analysis of the inherent properties of adsorbate and adsorbent systems (i.e. equilibrium isotherm, adsorption kinetics, shape of breakthrough curves, etc.) and simulation results. These rules included the selection of adsorbent, particle size, bed size, bed configuration, purge volume, pressure equalization and vacuum swing adsorption. Results of two case studies were presented to verify the rules proposed in this preliminary study.

Chung *et al.* (1998) also proposed a model to evaluate the performance of PSA systems. The basic steps in PSA systems were categorized into adsorption and desorption steps. Each step was mathematically modelled under the assumption of adsorption equilibrium in a batch mode. The batch model provided detail information on the relation between compositions of the feed and the product which can be used in the design of PSA systems just like the x-y diagram in liquid-vapor equilibrium processes. It could also be used in the design of bed couplings through recycle and cascade of its product. Even though the proposed evaluation model cannot predict the performance of the kinetically-controlled system, it can be used as a screening tool in adsorbent selections and process comparisons at the early design stage for PSA systems.

Simo *et al.* (2007) proposed a general package for the simulation of a cyclic PSA process. The system of partial differential equations was solved via method of lines using stiff equation integration package. Parameters for the model were based on the data from an operating plant as well as data from other literatures. For the ethanol production technology the proposed model provided a fundamental understanding of the dynamics of the cyclic process and effects of some operating parameters. The study examined the effects of the feed stream temperature, duration of the purge step, feed water concentration and pressure ratio on the performance of the de-watering process.

The results showed that the increase of the feed stream temperature could improve the quality of the product. Choosing a longer purging period had also favorable effect on the performance of the PSA unit. It was also suggested that further process intensification can be achieved by operating at higher pressure ratio by increasing the feed stream pressure and/or decreasing the regeneration pressure. It was shown that there is a possibility to operate the PSA unit with higher water content in the feed stream after proper adjustment of operating parameters according to above-mentioned recommendations.

In addition to the aforementioned works, there are researches proposed by Ahn and Brandani (2005), Choong *et al.* (2002), Jiang *et al.* (2003), Kvamsdal and Hertzberg (1997) and Smith and Westerberg (1992) which specifically developed new models and methods for accurate simulation of cyclic adsorption. These papers proposed models which were based on numerical method aiming not only on the simulation of the cyclic adsorption process but also on the optimization of PSA systems in a view of acceleration of cyclic steady state convergence. However, the proposed algorithm in these researches may need further development before proving to be suitable for processes that converge very slowly towards cyclic steady state or for processes which involve low concentration of adsorbate or purification using PSA.

Cruz *et al.* (2003) developed an innovative analysis strategy and an optimization procedure with the purpose of design, evaluation and optimization of small- and large-scale units of cyclic adsorption processes using the classical Skarstrom's cycle: pressure swing adsorption (PSA) and vacuum swing adsorption (VSA). The system of partial differential equations of the dynamic simulator model was solved using a numerical technique based on an adaptive multiresolution approach, thus ensuring stability and accuracy. The simulator provided models for the multiple phenomena involved in fixed-bed adsorption: pressure drop, mass transfer resistance and energy balance.

An extended parametric analysis was presented for the particular case of oxygen production from air by PSA and VSA in terms of influence of the normalized purge flow rate, the high and low pressure values, dimensionless pressurization time, dimensionless production time, pressure drop and temperature in the bed.

Tanaka and Otten (1987) used cracked grain corn as adsorbent to upgrade aqueous alcohol to anhydrous ethanol using a packed bed adsorption process. A 0.35 meter diameter by 3 meter dehydration column was designed and constructed on the basis of data obtained in series of bench-scale experiments. The resulted showed that grain corn could upgrade 91% ethanol to 99% ethanol at a rate of about 0.20 L/min. The capacity of the corn bed in the prototype was lower than expected from the bench scale experiments, which was attributed to the significant thermal effect of the heat of adsorption. The performance of the prototype was modeled mathematically using a one-dimensional dispersive-convective description of the bed. The model was observed to fit the experimental data well in the regions where heat effects were not pronounced, and showed a systematic departure in the no-isothermal regions.

Design and optimization of pressure swing adsorption systems with parallel implementation were proposed by Liang *et al.* (2005). It was suggested that the process was distributed in nature, with spatial and temporal variations and was mathematically represented by partial differential equations (PDEs). After a start-up time, the system reaches cyclic steady state (CSS), at which the conditions in each bed at the start and end of each cycle are identical, revealing normal production. A Newton-based approach with accurate sensitivities was implemented to directly determine cyclic steady states with design constraints. It was claimed that the simultaneous tailored approach could incorporate large-scale and detailed adsorption models and was more robust and efficient than competing optimization methodologies. The sensitivity calculation was parallelized to improve the computational efficiency and achieved a close-to-linear speed up rate.

Serbezov (2001) investigated the effects of several process parameters on the length of the mass transfer zone (MTZ) during product withdrawal in equilibrium controlled PSA operations. The process parameters under consideration were the adsorbent selectivity, the initial MTZ length, the product purity, and the adsorption pressure. For locally equilibrated PSA processes the analytical solution for binary mixtures was used to develop analytical expressions for the dependence of the MTZ length on the above-mentioned parameters.

For equilibrium controlled PSA process with the modest mass transfer limitations the evolution of the MTZ length during product withdrawal was examined through numerical simulations using a liner driving force (LDF) model. It was found that the length of the MTZ during product withdrawal was strongly affected by the adsorbent selectivity when the selectivity was below four, and by the initial MTZ length. The length of the MTZ during product withdrawal is modestly affected by the adsorbent selectivity when the selectivity was above eight, and by the product purity. However, it was claimed that the length of the MTZ during product withdrawal was not affected at all by the adsorption pressure for locally equilibrated PSA processes. For PSA processes with modest mass transfer limitations the length of the MTZ during product withdrawal was only mildly affected by the adsorption pressure.

Rakshit *et al.* (1993) studied the preferential adsorption of water in the vapor phase by lignocellulosic residues for the production of anhydrous ethanol. Rice straw, microcrystalline cellulose powder (MCCP) and bagasse were the lignocellulosic residues used as adsorbents. Starting with an ethanol concentration of 80-90% a final concentration above the azeotropic concentration was obtained. Furthermore, an energy analysis of the process was made and a possible explanation of phenomena was suggested. However, it was mentioned that further fundamental work would have to be done for scaling up the preferential adsorption system before it could be used for the production of gasohol type liquid fuels.

Chang *et al.* (2006) measured the adsorption isotherms of water vapor on cornmeal and the breakthrough curves at 82-100 °C in a fixed-bed apparatus for ethanol dehydration. Using the water isotherms measured and fitting the experimental data to fixed-bed model for breakthrough curve, the effective diffusivity of water was obtained. The effective diffusivity was estimated and used to predict breakthrough curves at other adsorption conditions through the model of Klinkenberg. The model could be successfully used for the prediction of breakthrough curves at different superficial velocity and different bed depth, but could not predict well the breakthrough curves for different vapor concentration. The analysis of mass-transfer resistance indicated that water adsorption on cornmeal was controlled by the internal mass-transfer resistance for both the low and high velocity at the end of the breakthrough curves.

Many mass transfer kinetic models were used to study varying pressure steps of a PSA cycle, namely pressurization and blowdown steps, by Chahbani and Tondeur (2000). It was shown that the choice of an appropriate model to account for intra-particle diffusional limitations was essential to simulate accurately PSA processes. It was demonstrated that, besides mathematical approximations (parabolic profile within the particle), a very important factor that can affect simulation results remarkably was the correctness of the mass transfer kinetic model when regarded as being a mass balance for the adsorbent particle. In fact, neglecting intra-particle gas phase led to erroneous simulations. Some models widely used in this literature, such as the classic linear driving force (LDF) and the solid diffusion models prove inadequate. It was recommended to use pore diffusion model as well as new version of the solid diffusion model to get reliable predictions.

Kearns and Webley (2006 A and 2006 B) proposed series of studies on modeling and evaluation of dual-reflux pressure swing adsorption cycles. It was suggested that Dual-reflux pressure swing adsorption (DR-PSA) systems represented new options for producing two pure products from binary gas mixtures using adsorption. Within the constraint of DR-PSA, there were several options: feed to the low- or high-pressure bed and equalize, repressurize and blowdown with either the weakly or strongly adsorbed gas (opposite ends of the adsorption column). Each of these options led to different flow sheets and resulted in different system performance, in particular productivity and work consumption tradeoff. In part I of this two part study the author formulated method of characteristics models for all of the dual reflux cases – in several cases new dual reflux models were developed which were yet to be reported. In part II, the power and productivity tradeoffs of all the dual reflux cycles developed in Part I were examined. It was found that the concentration of heavy component in the feed is primary variable that influences the choice of dual-reflux configurations. Feed to the high-pressure bed and equalization, pressurization and blowdown with the strongly adsorbed component was favored at low concentrations of heavy component in the feed. Feed to the low-pressure bed and equalization, pressurization and blowdown with weakly adsorbed component was favored for high concentrations of heavy component in the feed gas. For highly selective adsorbents, the differences between the work-productivity tradeoff for the

four configurations were quite distinct, becoming less distinct as the ease of separation decreased.

Ratkai *et al.* (2008) parameterized a new effective pair potential for the prediction of the adsorption of mixtures of water and methanol or ethanol in zeolite NaA. The pressure dependence of the adsorption properties such as equilibrium amount of adsorption and isosteric heat of adsorption were calculated at 378 K by molecular simulations. Significantly higher adsorption selectivities were found for water in a wide range of pressure as compared with previous simulation results. The verification of the new model was made by calculating also some structural characteristics of the system. It was also suggested that the increased degree of water adsorption at high alcohol contents may also had a strong influence on the diffusion contribution to the separation efficiency of the model membrane through hindering the window blockage by the larger alcohol molecules inside the membrane.

Huang *et al.* (2008) reviewed separation technologies in current and future biorefineries. It was claimed that biorefineries processed bioresources such as agriculture or forest biomass to produce energy and a wide variety of precursor chemicals and bio-based materials, similar to the modern petroleum refineries. Industrial platform chemicals such as acetic acid, liquid fuels such as bioethanol and biodegradable plastics such as polyhydroxyalkanoates could be produced from wood and other lignocellulosic biomass.

Biorefineries used a variety of separation methods often to produce high value co-products from the various feed streams. This literature provided a critical review of separation technologies related to biorefining including pre-extraction of hemicellulose and other value-added chemicals, detoxification of fermentation hydrolyzates, and ethanol product separation and dehydration was presented. For future biorefineries, extractive distillation with ionic liquids and hyperbranched polymers, adsorption with molecular sieve and bio-based adsorbents, nanofiltration, extractive-fermentation, membrane pervaporation in bioreactors, and vacuum membrane distillation hold significant potential and great promise for further investigation, development and application.

Al-Asheh *et al.* (2004) assessed the potential use of new biobased adsorbents and different types of molecular sieve in the separation of the ethanol-water azeotrope. Molecular sieves of type 3A, type 4A, and type 5A and biobased adsorbents such as natural corncobs, natural and activated palm stone and oak, were used in this research. Each of these adsorbents was packed in a column, which was surrounded by a heating jacket. The jacket temperature was maintained constant in an attempt to maintain the packed-column at constant temperature. The water concentration of ethanol in the flask was constant at the beginning of the experiment, it varied with time due to boiling.

The breakthrough curves of water sorption on these adsorbents at different water contents showed that among the molecular sieves examines, type 3A molecular sieves gave the best separation of the ethanol-water system and among biobased adsorbents examined, natural palm stone was the best. The Guggenheim, Anderson, and De Boer (GAB) model at different water contents represented the isotherms for water sorption on molecular sieves and biobased adsorbents. In addition, the surface area of adsorbents and maximum water uptake were calculated. Type 3A molecular sieves were determined to have the largest surface area and the highest value of water uptake compared with the other biobased adsorbents.

Lu *et al.* (2007) the grand canonical Monte Carlo (GCMC) simulation study on the separation performance of zeolites (MFI, MOR, CFI, and DON) and carbon nanotubes (CNTs) to ethanol-water mixtures was reported. The calculation was performed with different bulk percentage under the ambient temperature and pressure. The results showed zeolites preferred water to ethanol and could be used for ethanol dehydration. Only water could enter CNT55, but of other CNTs, because the CNT is more hydrophobic than zeolite, the selectivity of CNTs to ethanol is larger than 1, and CNT77 was very fit to condense dilute ethanol solution. CNT77 showed excellent performance for its special nanoscale. It preferred ethanol to water in all fraction range.

Ding *et al.* (2002) introduced an alternative method for determining the optimum periodic state of an adsorption cycle. The traditional method for determining a periodic state (cyclic steady state) of a mathematical model of an adsorption cycle

involves simulating a process through successive cycles until the solution is not changing significantly from cycle to cycle. Optimization is then carried out by exploring the solution space by varying parameters and determining several periodic states until an optimum or near-optimum solution is found. This paper proposed an approach which was based on determining a periodic state directly rather than by simulating successive cycles.

For optimization, an objective function was introduced into the equation set. The error in minimizing this objective function was driven to zero at the same time that errors in meeting the periodicity requirement and constraints were driven to zero. Thus, the first periodic state found was an optimum one. Moreover, an optimum feed temperature was found for the temperature swing adsorption cycle. The researchers then further described several enhancements to accelerate the direct determination of the periodic states of fixed bed adsorption cycles (Ding and Le Van, 2001).

Gorbach *et al.* (2004) analyzed the adsorption of water vapor on zeolite 4A. Both equilibrium and kinetics were examined. The equilibrium was measured with a static-volumetric method in a wide range of partial pressure and temperature and was modeled by several conventional approaches and a new type isotherm model, which fitted the obtained data best. Kinetics were determined by measuring breakthrough curves. The breakthrough curves were matched by a detailed model based on a modified linear driving force (LDF) approximation for the mass exchange. An analytic expression for the corresponding LDF-coefficient was designed in order to describe its dependency on water concentration, temperature and pressure. For the practical range of operating conditions the dependency on concentration can be described by the nonlinearity of the adsorption isotherm. The dependency on temperature and pressure corresponds to that of molecular diffusion.

Liu *et al.* (1998) compared three different finite-difference routines for solving the nonlinear, coupled, partial differential and algebraic equations that describe pressure swing adsorption processes. A successive substitution method (SS), a block LU decomposition procedure (BLUD), and the method of lines approach with adaptive time stepping (DASSL) were used to simulate and compare the computation times required to reach the periodic state for two different PSA systems: PSA-air

drying and PSA-solvent vapor recovery. For both systems, the results showed that DASSL and BLUD were also very robust and accurate, as nearly identical bed profiles were obtained from both methods under both transient and periodic state conditions.

According to Todd and Webley (2005), simulation of cyclic adsorption processes for gas separation relies on accurate models of the bed pressure drop during dynamic pressurization, depressurization, and breakthrough steps. This was especially true for rapid pressure swing adsorption (RPSA), where large gas flows can cause significant changes in the axial pressure gradient through the bed, influencing process performance. Under these conditions, there was some question as to the validity of conventional steady-state models used to represent the dynamic, rapidly changing pressures. In this paper, the ability of the steady-state Ergun equation to represent pressure drop under dynamic adsorbing and nonadsorbing conditions was tested. The Ergun equation accurately reproduced dynamic depressurization and breakthrough pressure profiles using values of $K_{viscous}$ and $K_{kinetic}$ (the two Ergun parameters) determined experimentally from the steady-state flow of a variety of gases through a packed bed of LiLSX pellets.

The full momentum equation was also tested, and errors of <0.1% were observed between the Ergun equation and the full momentum balance under dynamic conditions for a non-adsorbing packed bed. The observations and simulations suggested the Ergun equation could be reliably used to reproduce experimental profiles under dynamic adsorbing conditions where high gas flow result.

Many authors have pointed out that using 3A molecular sieve in a PSA system can potentially be very attractive for water adsorption from ethanol-water mixture, due to low energy consumption and low set up cost. They carried out a number of preliminary experiments and simulations, reaching the conclusion that PSA has the required specificity for the separation process under consideration. With the aim of carrying out these works one step forward, in the present study the behavior of a widely available commercial zeolite will be investigated and the most suitable one will be selected for water-ethanol separation. In particular, with the properly engineered separation process, the equilibrium behavior of the selected zeolite and the

sequential steps of the PSA process will be proposed. An attempt will be made to give a unifying description of the experimentally obtained results in terms of the theory of adsorption and, furthermore, the water-ethanol adsorption isotherms can be predicted.